In situ Atomic Force Microscopy in the study of Electrogeneration of polybithiophene on Pt electrode

Available online at www.sciencedirect.com
SCIENCE DIRECT®
Electrochimica Acta 50 (2005) 1497–1503
ELECTROCHIMICA Acta
www.elsevier.com/locate/electacta

In situ atomic force microscopy in the study of electrogeneration of polybithiophene on Pt electrode

M. Innocenti[a], F. Loglio[a,1], L. Pigani[b,1], R. Seeber[b,*,1], F. Terzi[b], R. Udisti[a]

[a] *Dipartimento di Chimica, Università degli Studi di Firenze, via della Lastruccia 3, 50019 Sesto Fiorentino (FI), Italy*
[b] *Dipartimento di Chimica, Università degli Studi di Modena e Reggio Emilia, via G. Campi 183, 41100 Modena, Italy*

Abstract

Electrochemical AFM technique has been used for the in situ study of the electrogeneration-deposition process of polybithiophene at varying the polymerisation conditions, such as supporting electrolyte, i.e., $LiClO_4$ or tetrabutylammonium hexafluorophosphate, and polymerisation procedure, i.e., either potentiostatic or potentiodynamic method. In order to better follow the evolution of the morphology of the deposit, particularly during the early stages of the polymer film growth, a suitable home-made electrochemical cell has been used.

Keywords: Atomic force microscopy; Conducting polymers; Polythiophene; Electrochemical polymerisation

1. Introduction

Conducting polymers (CPs) are particularly interesting materials for a number of applications, ranging from batteries to molecular electronic devices [1–8]. Among CPs, polythiophenes stand out thanks to peculiar electronic, optical, and electrochemical properties. In particular, as regards our principal field of interest, they are very appealing modifiers of the electrode surface when aiming at developing amperometric sensors.

Electrochemistry has played a meaningful role in the preparation and characterisation of these novel materials, since electrochemical techniques are especially suitable for carrying out syntheses under controlled conditions and for tuning a well-defined oxidation state or oxidation level. Films of these materials on electrodes can be easily set either in the insulating or in the conductive state, exhibiting correspondingly different electrical, optical, and chemical properties. In comparison with the impressive amount of work carried out on the synthesis of new CPs, not so much is known about their electronic and molecular structure, as well as about the morphological modifications they undergo when switching from insulating to conductive state and vice versa: these changes are reasonably fairly important in order to give a rationale to the factors affecting the switch itself and the related conducting properties. The characterisation and the performances of a CP, in fact, are critically linked to the surface status, due to the interfacial character of the electrode processes. Furthermore, a number of efforts have been directed towards the development of suitable and 'ordered' structures in CPs, because of the possible improvement in the conductivity achieved by growing films with controlled morphology.

The need for a deeper understanding of these systems requires the use of ultra-high resolution techniques, such as Scanning Probe Microscopies (SPM) [9–13]. Among the various SPM techniques, Scanning Tunneling Microscopy (STM) and Atomic Force Microscopy (AFM) have been extraordinarily useful for obtaining images of the electrode surface directly, also under a controlled polarisation potential [14–19]. In particular, AFM and electrochemical AFM have been extensively used in the study of the polymer deposition process at varying the polymerisation conditions, such as type of substrate, solvent, supporting electrolyte, temperature, etc., as well as in the investigation of the polymerisation procedure [20–30]. Among CPs, polypyrrole (PPy) has been widely studied using SPM techniques. A large amount of re-

* Corresponding author. Tel.: +39 059 2055027; fax: +39 059 373543.
E-mail address: seeber@unimore.it (R. Seeber).
[1] ISE member.

0013-4686/$ – see front matter © 2004 Elsevier Ltd. All rights reserved.
doi:10.1016/j.electacta.2004.10.034

search has been published about the mechanism of the initial growth and the resulting surface morphology, as a function of the electrosynthesis conditions, as well as about the properties of the doped state as a function of the polymer morphology [21–23,31–33]. These studies show partial agreement as to the proposed dependence of morphology over growing conditions of the CP. First, STM studies on polythiophenes appeared in the nineties [34–36]. AFM investigation of the early stages of the electrochemical deposition of polybithiophene from propylene carbonate solution revealed that polymer deposition starts with formation of separate nuclei and that the morphology of the film is independent of the deposition current intensity, which has been tentatively explained by the poor solubility of the oligomers in propylene carbonate [26].

In this paper, we present the results of an in situ investigation of the early stages of electrochemical generation-deposition on the Pt electrode of polybithiophene (PBT) films from acetonitrile solution. The choice of bithiophene, instead of thiophene, as the starting dimer has been suggested by literature reports, which claim enhanced regularity and stability of the film obtained [37,38]. Owing to the scope of the work, it was particularly urgent to use a proper cell geometry, so that we developed a suitable home-made cell for the in situ AFM measurements. We compare the results obtained by working with two different supporting electrolytes, i.e., $LiClO_4$ or tetrabutylammonium hexafluorophosphate ($TBAPF_6$). Different counterions may have different interactions with the radical cations of the starting dimer and of the growing chain, influencing the polymerisation rate and the deposit growth efficiency and packing. Moreover, different supporting electrolytes can heavily affect the swelling properties of an already formed CP deposit. Furthermore, an examination of the influence of the electrosynthetic method (i.e., either voltammetric or potentiostatic method) on the surface morphology of the PBT film has been also made. Preliminary studies performed on various polythiophenes had put in evidence that systematic in situ AFM studies can offer a direct view of these aspects.

2. Experimental

2.1. Chemicals

The dimeric starting compound bithiophene (BT) and the supporting electrolytes, $LiClO_4$ and $TBAPF_6$, were Fluka puriss. products; they were used without further purification. Anhydrous (water content < 0.05%), acetonitrile solvent, packaged under nitrogen, was from Aldrich, 99.8% pure. No attempt was made to remove the oxygen present due to contact with air, during the synthesis of PBT, except for flowing N_2 (>99.99% pure) above the solution.

2.2. Electrochemical and AFM apparatus

Polymerisation and electrochemical experiments were performed using an electrochemical cell (Scheme 1A) designed by us. The cell body was made of Voltalef® (Fluorten, Bergamo, Italy), and the 1.5 cm inner diameter was adapted to the standard Molecular Imaging sample plate, by means of two screws.

The working electrode was a 0.5-mm thick polycrystalline platinum foil (Alfa Aesar), with 1.5 cm × 2 cm dimension. The electrode surface was polished repeatedly with finer and finer grade alumina powder (Buehler Micropolish II), from 0.3 μm to 0.05 μm. After polishing, the electrode surface was soaked in pure water for about 30 min and then rinsed with fresh water. The water used was distilled twice, the first time from alkaline permanganate, always discarding the distillation heads.

Scheme 1 B shows the experimental apparatus for in situ measurements. The Pt foil constitutes the bottom of the cell and Pt wires are used as auxiliary and pseudo-reference electrode, respectively. The Pt wire used as auxiliary electrode is circularly wrapped, positioned close above the surface of the platinum foil, which allows us to obtain a uniform growth of the polymer deposit. Only to give an idea of some reported potential values, in cyclic

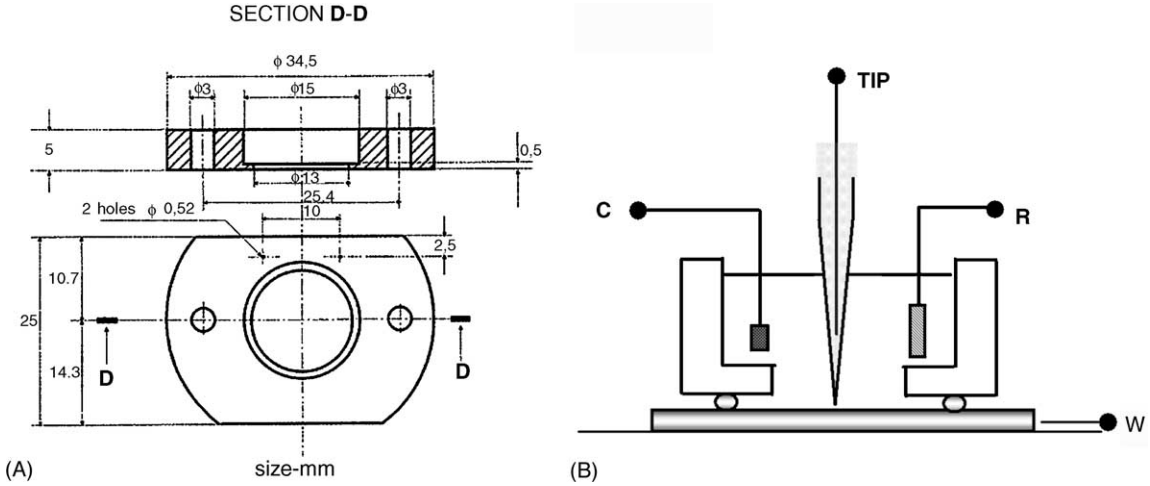

Scheme 1. Schematic view of the cell used for in situ AFM electrochemical measurement (A) upper view and (B) side view.

voltammetric tests performed in a conventional cell using the Pt wire as a reference electrode, the $E_{1/2,r}$ measured on the anodic–cathodic peaks system recorded for the ferrocene/ferrocinium (Fc^+/Fc) reversible couple in acetonitrile solvent resulted at ca. +0.18 V, with minimum shift from $LiClO_4$ to $TBAPF_6$ supporting electrolyte. The Pt wire was polished according to a strictly similar procedure before each one of these tests and before every AFM electrochemical experiment.

Topography was measured in situ in the described cell, using a Molecular Imaging AFM instrument (PicoSPM, Molecular Imaging) operating in contact mode, with a commercial Si_3N_4 cantilever (Nanosensors, Wetzlar-Blankenfeld). The surfaces of bare Pt and of polymeric deposits were characterised by non-filtered 512 × 512 pixel images with areas ranging from 1 μm × 1 μm to 25μm × 25 μm. These images were elaborated by the commercial program Visual SPM IDL 5.3.

Different methods for roughness evaluation are commonly used, depending on the quantity that best describes the system. We preferred using the Root Mean Square Roughness, R_{RMS} [39,40], which is the estimate of the standard deviation of the bidimensional Gaussian-type distribution of heights around the mean value of the collected points.

3. Polymer growth

$LiClO_4$ and $TBAPF_6$ were chosen as representative supporting electrolytes among those allowing only p- or both p- and n-doping of PBT to occur, respectively. They are also known to exhibit quite a different behaviour with respect to the residual charge phenomenon [41,42], which suggests different interaction of ClO_4^- and PF_6^- ions with the charged polymer both during polymerisation and charge–discharge processes.

Fig. 1 shows typical cyclic voltammograms recorded during BT oxidation in a CH_3CN solution containing 0.01 M BT and 0.1 M supporting electrolyte. The curves are recorded using a conventional size Pt electrode, which allows us to obtain clearer voltammograms, better evidentiating differences in the potential peak position of monomer oxidation for different supporting electrolytes and to refer the response to a proper reference, such as $E_{1/2}$ of the ferricinium/ferrocene couple. The voltammograms shown are both characterised by irreversible oxidation peaks, ca. 0.2 V far form each other, located at ca. +0.8 V and +1.0 V, respectively, with respect to $E_{1/2,r}$ of the Fc^+/Fc redox couple and at ca. +1.0 V and +1.2 V with respect to the Pt wire pseudo-reference, respectively. On the basis of these voltammograms, the potential values for both potentiostatic and potentiodynamic growth in the solutions considered were chosen.

The choice of the conditions under which to grow the polymers to compare with each other as to a selected property constitutes a serious problem. In our case, the polymer is the same, but different electrolytes lead to different voltammetric responses, specifically as regards the potentials at which the monomer is oxidised and at which the charge–discharge process of the polymer takes place. A choice could be to operate under galvanostatic conditions, imposing an equal, low enough current value. However, notable differences arise in the compensation of the polarons on the polymer, due to the different resistance to the entrance of different counterions and different strength of the ionic couples formed. This implies the assumption of different potentials by the polymer deposit, which induces different behaviour with respect to the species in solution. We choose to work at controlled potential, not necessarily referred to the location of the relevant voltammetric peaks, which are a function of the potentiodynamic conditions under which they are recorded. We adopted quite an empirical criterium choosing values such that similar, very low currents flow, suitable to collect well comparable amounts of charge in equal times under the two different conditions. This also implies not to induce too much different charge densities on the growing polymers.

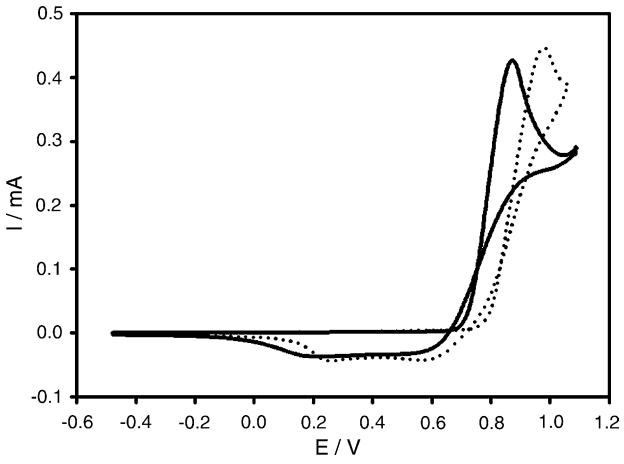

Fig. 1. Voltammetric curves relative to 10 mM BT monomer oxidation: CH_3CN solution, 50 mV s^{-1} potential scan rate. Solid line: in the presence of $LiClO_4$; dotted line: in the presence of $TBAPF_6$. Potential are referred to the Fc^+/Fc redox couple.

3.1. Potentiostatic growth

The growth of the PBT deposit at the electrode surface in the presence of $LiClO_4$ was carried out at +0.57 V versus the Fc^+/Fc redox couple. In these conditions, working at the foot of the oxidation peak of the monomer, the synthesis was slow enough to follow the PBT formation step by step. Subsequent AFM images were taken, at a potential corresponding to the discharge of the polymer, i.e., at −0.58 V versus Fc^+/Fc redox couple, immediately after subsequent growths of 1 min. In this way, subsequent images well account for the details of the PBT growth; AFM images of the bare electrode surface were also recorded. Fig. 2 only reports images selected among all those collected in order to give best account of the 'evolution' of the surface profile of the deposit.

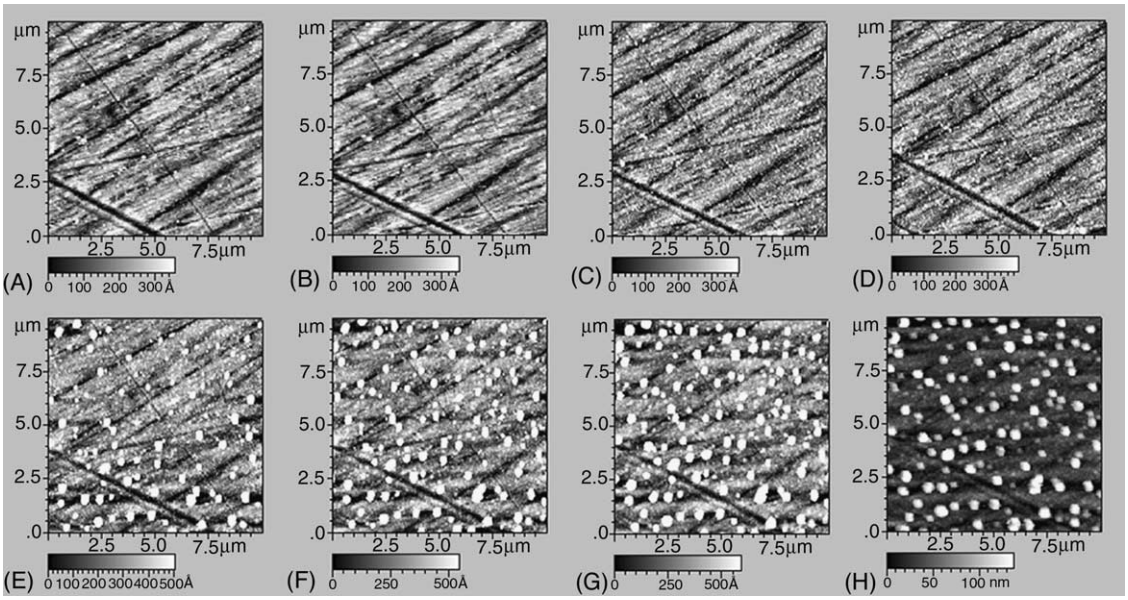

Fig. 2. AFM images of PBT grown on polycrystalline Pt electrode during various stages of growth at +0.58 V vs. Fc^+/Fc redox couple in the presence of $LiClO_4$ supporting electrolyte. (A) bare electrode; after starting the electropolymerisation by: (B) 1′; (C) 6′; (D) 7′; (E) 8′; (F) 13′; (G) 18′; (H) 23′.

At a first sight, the images reported reveal that the depth of the slight scratches present on the bare substrate (see Fig. 2A) progressively fade at increasing amounts of deposited polymer. The PBT film consists of a homogeneous distribution of globular features (grains or nodules), which can be easily recognised over the surface, revealing that the polymerisation proceeds through preferential growth of initially formed 'active' nuclei. At quite an early stage, the PBT clusters fuse into one another covering the whole electrode surface.

In order to gain deeper insight on nucleation and growth processes during PBT film formation, R_{RMS} values were computed and an analysis of the clusters' size was performed. Table 1 also reports the value of a further, commonly used parameter, i.e., of Δh, representing the difference between maximum and minimum deposit thickness within the set of images collected.

The reported values could be taken as well representative of a reproducible situation, being averaged over repeated tests. R_{RMS} and Δh values relative to the images in Fig. 2A–C confirm that the polymer grows at first on the substrate defects, represented in this case by the scratch lines on the bare Pt surface. Then, the number of PBT clusters increases as the deposition goes on: at the same time, the PBT clusters previously formed increase in both height and width. The regularity of the grain shape, size, and height can be supposedly accounted for by formation of grains according to a mechanism of progressive nucleation, like that described in [22]. This suggests that the deposit grows through the formation of new nuclei and that at the same time preferential deposition of chains at nucleation centres, according to a three-dimensional growth mechanism, occurs. It should be noticed that individual grains are spherical in shape, with an average diameter of 400 nm, as shown in Fig. 2H.

In order to relate the change in the polymer film formation to the nature of the counterion, we also prepared PBT films using $TBAPF_6$ as the supporting electrolyte. As a first consideration, we can notice that in this case we should apply a more anodic potential (+0.77 V versus Fc^+/Fc redox couple) in order to make the growth to occur at a comparable speed. A very high number of small nucleation centres appears on the substrate surface and, as the growth proceeds, their dimension increases in a non-homogeneous way, resulting in a final non-uniformity of the polymer grains. Also in this case,

Table 1
R_{RMS} and Δh values relative to images reported in Fig. 2

Image in Fig. 2	R_{RMS} (nm)	Δh (nm)
A	9.1	96
B	8.5	81
C	9.6	130
D	10.6	143
E	22.5	233
F	27.2	254
G	31.3	261
H	35.4	261

Table 2
R_{RMS} and Δh values relative to images reported in Fig. 3

Image Fig. 3	R_{RMS} (nm)	Δh (nm)
A	10.8	120
B	10	99
C	12.3	200
D	14.9	208
E	16	215
F	18.2	224
G	19	236
H	21	254

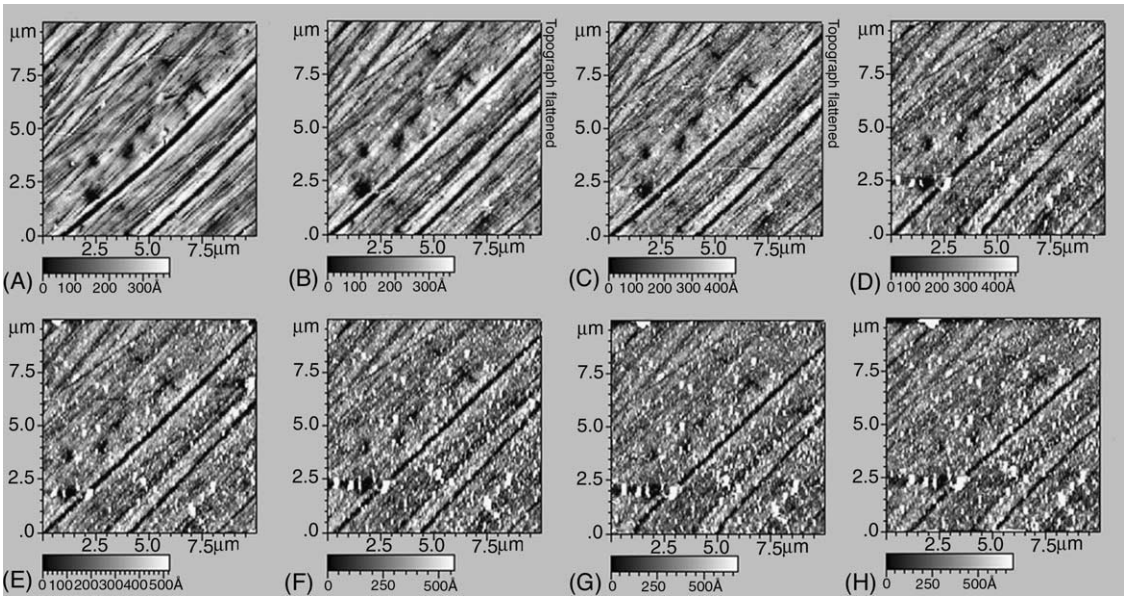

Fig. 3. AFM images of PBT grown on polycrystalline Pt electrode during various stages of growth at +0.77 V vs. Fc^+/Fc redox couple in the presence of $TBAPF_6$ supporting electrolyte. (A) Bare electrode; after starting the electropolymerisation by: (B) 1′; (C) 6′; (D) 7′; (E) 8′; (F) 13′; (G) 18′; (H) 23′.

R_{RMS} and Δh values were computed, and reported in Table 2 (Fig. 3).

The trend of the R_{RMS} and Δh values during the progressive growth of the deposit, suggests that the three-dimensional growth mechanism prevails in the first stages of polymer deposition, while, after that a compact polymer layer has formed on the Pt substrate, the bi-dimensional growth is preferred [22,23].

Finally, Fig. 4 shows clearly the differences in the final three-dimensional morphology of the PBT deposit, grown potentiostatically in the presence of the two different supporting electrolytes. In order to compare and emphasise the differences between PBT cluster sizes, the *z* scale of the cross-sections were kept equal in the two images. Apart from the well evident differences in the cluster heights, we can also compare the diameter (ϕ) of the largest grain in the two cases, which resulted of 800 nm in the presence of $LiClO_4$ and of 1100 nm in the presence of $TBAPF_6$. As already mentioned, differences between the two supporting electrolytes could be due to the action played by the counterion during the polymer growth and by the whole supporting electrolyte during the doping process, since polymerisation occurs at potentials at which the polymer already deposited is conducting, i.e., doped and including anions.

The trend depicted by the AFM images during the potentiostatic polymerisation of PBT in the presence of $LiClO_4$ or $TBAPF_6$ is well consistent with the information obtained in previous studies. In particular, a recent work [43] performed by us on *S*-alkyl substituted PBTs using the Electrochemical Quartz Crystal Microbalance put in evidence that $LiClO_4$ assures a higher rate of polymerisation and of deposit growth than $TBAPF_6$ does. This has been attributed principally to dif-

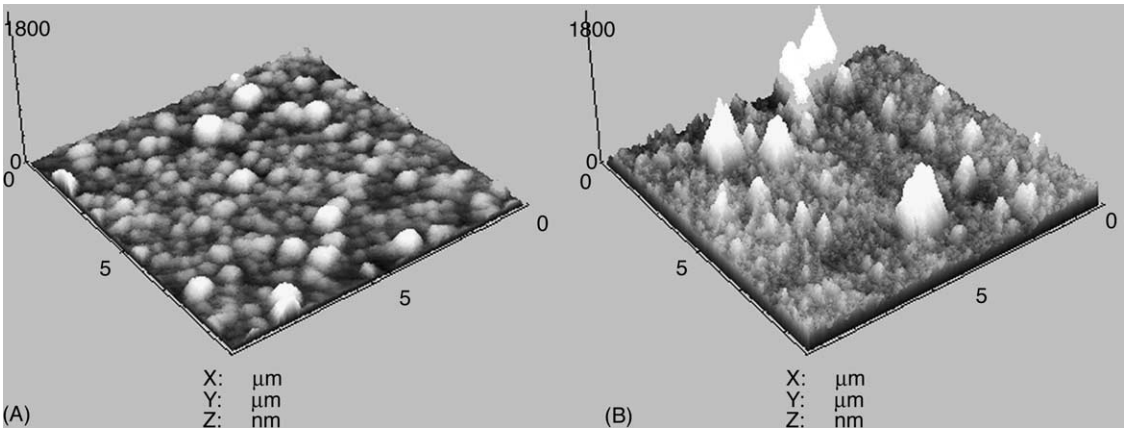

Fig. 4. Three-dimensional images after 23 min of electropolymerisation in the presence of (A) $LiClO_4$ supporting electrolyte at 0.58 V vs. Fc^+/Fc redox couple; (B) $TBAPF_6$ supporting electrolyte at 0.95 V vs. Fc^+/Fc redox couple.

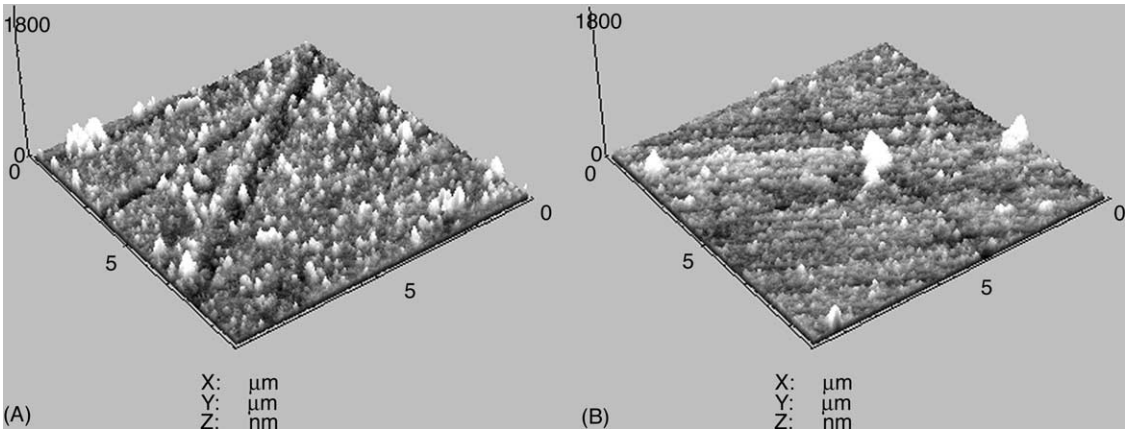

Fig. 5. Topographic in situ AFM images of PBT grown potentiodynamically in a 0.01 M dimer, 0.1 M (A) $LiClO_4$ and (B) $TBAPF_6$, CH_3CN solution.

ferent interactions of the radical cationic centre on the starting dimer and on the growing chain, with the anionic counterion. Nevertheless, PF_6^- assures higher charge efficiency with respect to deposit formation.

3.2. Potentiodynamic growth

Electropolymerisation of PBT was also carried out by potentiodynamic route in the potential range between −0.58 V and +1.02 V versus Fc^+/Fc redox couple. AFM images were typically taken after eight potential scans at 50 mV s^{-1}. Since the morphology of the PBT film surface depends on many different parameters that are difficult to control simultaneously when the preparation is performed by voltammetric method, our goal was not to follow the growth from the first stages, but just that of looking at the morphology of the deposited film at subsequent voltammetric scans, up to a point at which quite similar pictures were collected.

Fig. 5 reports AFM images of the PBT film in the neutral form after potentiodynamic polymerisation in the presence of $LiClO_4$ or $TBAPF_6$ as supporting electrolytes. The PBT morphology with both supporting electrolytes appears very similar to that obtained by the potentiostatic route in the presence of $TBAPF_6$. It can be observed that, in addition to the numerous individual PBT nodules (as in the previous case) large features, in forms of non-regular patches, are also recognised on the electrode surface.

In order to estimate the surface roughness for the imaged samples, a roughness analysis was performed, leading to the results reported hereafter.

(A) RMS = 26.2 nm; Δh = 405 nm—$LiClO_4$ supporting electrolyte;
(B) RMS = 26.9 nm; Δh = 458.6 nm—$TBAPF_6$ supporting electrolyte.

It is evident that under these conditions of growth the nature of the supporting electrolyte used does not influence the polymer morphology to a notable extent, except for a slightly higher number of big clusters in the case of $LiClO_4$ supporting electrolyte.

Differences between these morphologies and the previous ones, observed by potentiostatic method, can be attributed to an association process between the polymer grains (nodules) observed for films grown by potentiostatic method. The fact that at each single anodic–cathodic scan the deposited polymer is allowed to discharge and possibly relax to lower potential energy over a relatively long time, rather that being continuously undergone to current flow and consequent formation of new polymer, may give explanation to the additional polymer transformation process involving partial grain association yielding bigger grains with non-uniform distribution.

4. Conclusions

Different morphologies are exhibited by PBT surfaces when following different polymerisation procedures. In particular, the potential step method allows better control of growth by AFM since the very early stages of the electropolymerisation process. In the potentiostatic growth, particularly evident differences in morphology are induced by the different nature of the salt used as the supporting electrolyte, more or less markedly favouring the packing of the polymer macromolecules to form the deposit. These differences might also be connected with the different behaviour of the polymer grown in the presence of the two different electrolytes, with respect to the ‘charge trapping’ phenomenon. Furthermore, based on the observations drawn out from AFM images taken during potentiostatic polymerisation, we concluded that PBT grains are formed progressively, which is characteristic of so-called progressive nucleation. The next step of our study will be the examination of the evolution of the morphology of PBT and other polythiophenes, such as poly[4,4′-bis(alkylsulphanyl)-2,2′-bithiophene]s and poly[3,4-ethylenedioxythiophene], when applying p- and n-doping potentials. This in order to possibly relate the swelling-compacting phenomena of the CPs with

the steric hindrance of the substituents on the polythiophene chain.

Acknowledgements

Financial support of MIUR (Rome), 'Ricerche di Interesse Nazionale', is acknowledged. We are indebted with Andrea Pozzi, Workshop of the Chemistry Department of the University of Florence, for manufacturing the AFM electrochemical cell.

References

[1] T.A. Skotheim (Ed.), Handbook of Conducting Polymers, Marcel Dekker, New York, 1986.
[2] M.E.G. Lyons (Ed.), Electroactive Polymer Electrochemistry, vols. 1 and 2, Plenum, New York, 1994.
[3] R.W. Murray (Ed.), Molecular Design of Electrode Surfaces, J. Wiley & Sons Inc., 1993.
[4] J. Heinze, in: Steckhan (Ed.), Topics in Current Chemistry, vol. 152, Springer, Berlin, 1990.
[5] R.W. Murray, in: A.J. Bard (Ed.), Electroanalytical Chemistry, vol. 13, Marcel Dekker, New York, 1984.
[6] J. Roncali, Chem. Rev. 92 (1992) 711.
[7] J. Roncali, J. Mater. Chem. 9 (1999) 1875.
[8] G. Inzelt, M. Pineri, J.W. Schultze, M.A. Vorotyntsev, Electrochim. Acta 45 (2000) 2403.
[9] W.J. Lorenz, W. Plieth (Eds.), Electrochemical Nanotechnology, Wiley-VCH, Weinheim, 1998.
[10] D. Bonnell (Ed.), Scanning Probe Microscopy and Spectroscopy, second ed., Wiley-VCH, Weinheim, 1998.
[11] R. Kellner, J.-M. Mermet, M. Otto, H.M. Widmer, Analytical Chemistry, Wiley-VHC, Weinheim, 1998.
[12] G.J. Leggett, in: J.C. Vickerman (Ed.), Surface Analysis, second ed., Wiley, New York, 1998.
[13] K.S. Birdi, Scanning probe microscopes, in: Applications in Science and Technology, CRC Press, 2003.
[14] H.K. Wickramasinghe, Acta Mater. 48 (2000) 347.
[15] N.J. Tao, C.Z. Li, H.X. He, J. Electroanal. Chem. 462 (2000) 81.
[16] R.W. Carpick, M. Salmeron, Chem. Rev. 97 (1997) 1163.
[17] A.A. Gewirth, B.K. Niece, Chem. Rev. 97 (1997) 1129.
[18] J.E.T. Andersen, J.-D. Zhang, Q. Chi, A.G. Hansen, J.U. Nielsen, E.P. Friis, J. Ulstrup, Trends Anal. Chem. 18 (1999) 665.
[19] R.M. Nyffeneger, R.M. Penner, Chem. Rev. 97 (1997) 1195.
[20] E.C. Venancio, C.A.R. Costa, S.A.S. Machado, A.J. Motheo, Electrochem. Comm. 3 (2001) 229.
[21] M. Suarez, R.G. Compton, J. Electroanal. Chem. 462 (1999) 211.
[22] B.J. Hwang, R. Santhanam, Y.-L. Lin, J. Electrochem. Soc. 147 (2000) 2252.
[23] B.J. Hwang, R. Santhanam, Y.-L. Lin, Electrochim. Acta 46 (2001) 2843.
[24] T. Hernandez-Perez, M. Morales, N. Batina, M. Salmon, J. Electrochem. Soc. 148 (2001) C369.
[25] M.J. Miles, W.T. Smith, J.S. Shapiro, Polymer 41 (2000) 3349.
[26] O.A. Semenikhin, L. Jiang, T. Iyoda, K. Hashimoto, A. Fujishima, Synth. Met. 110 (2000) 195.
[27] J. Ding, W.E. Price, S.F. Ralph, G.G. Wallace, Synth. Met. 110 (2000) 123.
[28] K.L. Mulfort, J. Ryu, Q. Zhou, Polymer 44 (2003) 3185.
[29] C.A. Mills, D. Lacey, G. Stevenson, D. Martin Taylor, J. Mater. Chem. 10 (2000) 1551.
[30] M.D. Levi, Y. Cohen, Y. Cohen, D. Aurbach, M. Lapkowski, E. Vieil, J. Serose, Synth. Met. 109 (2000) 55.
[31] J.N. Barisci, R. Stella, G.M. Spinks, G.G. Fallace, Electrochim. Acta 46 (2000) 519.
[32] J.M. Davey, S.F. Ralph, C.O. Too, G.G. Wallace, Synth. Met. 99 (1999) 191.
[33] R. Yang, D.F. Evans, L. Christensen, W.A. Hendrickson, J. Phys. Chem. 94 (1990) 6117.
[34] S.Z. Dong, Q. Cai, P. Liu, A.R. Zhu, Appl. Surf. Sci. 60 (1992) 342.
[35] T.L. Porter, S. Jeffers, G. Caple, B.L. Whecler, R. Swift, Surf. Sci. Lett. 238 (1990) L433.
[36] G. Caple, B.L. Wheeler, R. Swift, T.L. Porter, S. Jeffers, J. Phys. Chem. 94 (1990) 5639.
[37] T. Morgenstern, U. Konig, Synth. Met. 67 (1994) 263.
[38] M. Fujutsuka, R. Nakahara, T. Iyoda, T. Shimidzu, S. Tomita, Y. Hatano, F. Soeda, A. Ishitani, H. Tsuchiya, A. Ohtani, Synth. Met. 53 (1992) 1.
[39] J.D. Kiely, D.A. Bonnell, J. Vac. Sci. Technol. B 15 (4, July/August) (1997) 1483.
[40] M. Innocenti, S. Cattarin, F. Loglio, T. Cecconi, G. Seravalli, M.L. Foresti, Electrochim. Acta 49 (2004) 1327.
[41] S. Fletcher, J. Chem. Soc., Faraday Trans. 89 (1993) 311.
[42] H. Ding, Z. Pan, L. Pigani, R. Seeber, C. Zanardi, J. New Mat. Electrochem. Syst. 3 (2000) 337.
[43] L. Pigani, R. Seeber, F. Terzi, C. Zanardi, J. Electroanal. Chem. 562 (2004) 231.